ELSEVIER

Nuclear Instruments and Methods in Physics Research A 375 (1996) 21–25

NUCLEAR INSTRUMENTS & METHODS IN PHYSICS RESEARCH Section A

Dielectric-loaded free-electron maser in a stripline structure

M. Einat, E. Jerby*, A. Shahadi

Faculty of Engineering, Tel Aviv University, Ramat Aviv 69978, Israel

Abstract

Experimental results of a dielectric-loaded free-electron maser (FEM) oscillator in a stripline structure are presented. The table-top oscillator experiment employs a low-energy electron beam (8 keV, 0.5 A) and a folded-foil wiggler (2 cm period). The waveguide consists of dielectric slabs and metal striplines along the side walls of a rectangular tube. The metallic striplines protect the dielectric slabs attached to them from the electron beam, and support a quasi-TEM mode in the waveguide. The effective dielectric constant of the dominant odd quasi-TEM mode is measured as $\varepsilon_{\rm eff} \cong 8$. The oscillator operates in a frequency range of 3–5 GHz, in agreement with the tuning relation of the slow-wave dielectric-loaded free-electron maser.

1. Introduction

Free-electron lasers (FELs) are considered typically as *fast-wave* devices. They operate in the infrared regime and in shorter wavelengths, in free-space optical modes [1]. Longer wavelength devices, known as ubitrons or free-electron masers (FEMs), operate in the microwave and in the millimeter wave regimes in uniform waveguides which support fast-wave modes [2]. The tuning relation of the FEL-type interaction is

$$V_e \cong \omega/(k_z + k_w)\,, \tag{1}$$

where V_e is the longitudinal electron velocity, ω and k_z are the em-wave angular frequency and axial wavenumber, respectively, and $k_w = 2\pi/\lambda_w$ is the wiggler periodicity.

Several schemes of *slow-wave* FELs have been proposed and studied. These include the gas-loaded FEL [3] and the periodic-dielectric FEL [4]. Other devices which consist of wigglers and periodic structures are the efficiency enhanced FEL by slow RF field [5], and the traveling-wave FEM [6]. The latter was proposed as a synergism of the TWT and the FEL interactions. The Cherenkov maser is also considered as an FEL-type device which employs a dielectric waveguide without a wiggler [7–9].

The effects of dielectric loading on fast-wave interactions, such as the FEM and the cyclotron-resonance maser (CRM), are studied in Refs. [10–14]. While the dielectric loading improves the interaction bandwidth and efficiency, it also, on the other hand, introduces technical difficulties due to the vicinity of an isolating dielectric material and a high-energy electron beam.

The tuning relation of a dielectric-loaded FEL, assuming $k_z = \sqrt{\varepsilon_{\rm eff}}\,\omega/c$, where $\varepsilon_{\rm eff}$ is the effective dielectric constant of the medium, results from Eq. (1) as

$$\omega = V_e k_w/(1 - \sqrt{\varepsilon_{\rm eff}} V_e/c)\,. \tag{2}$$

Eq. (2) shows that the Doppler up-shift in the dielectric-loaded FEL might be considerably large for slow electrons near the Cherenkov synchronism ($V_e \approx c/\sqrt{\varepsilon_{\rm eff}}$).

In this paper we present experimental results of a dielectric-loaded free-electron maser (FEM) in a stripline structure. This waveguide supports a quasi-TEM mode in a wide range of frequencies and provides a metallic protec-

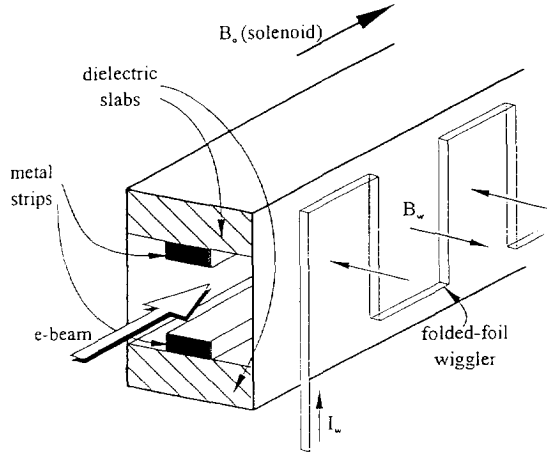

Fig. 1. The stripline waveguide structure.

* Corresponding author. Fax +972 3 6423508, e-mail jerby@taunivm.tau.ac.il.

SSDI 0168-9002(95)01197-8

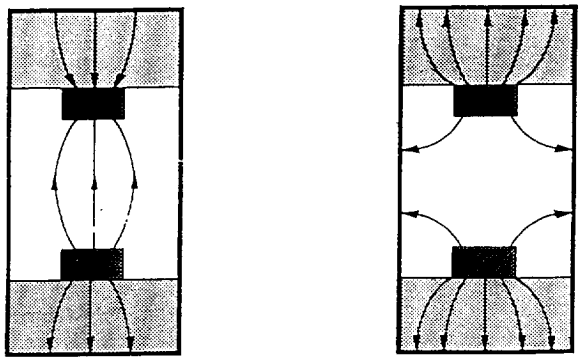

(a) Odd Mode (b) Even Mode

Fig. 2. Transverse field profiles of the odd (a) and even (b) quasi-TEM modes.

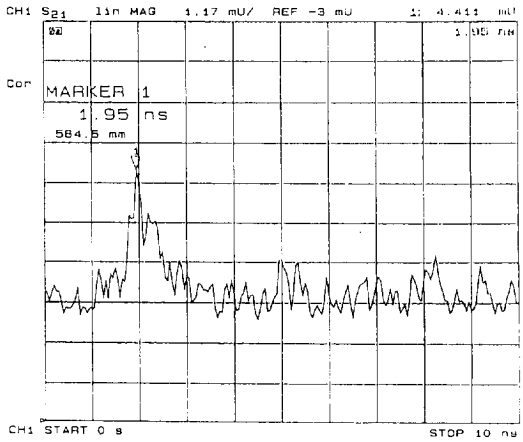

(a)

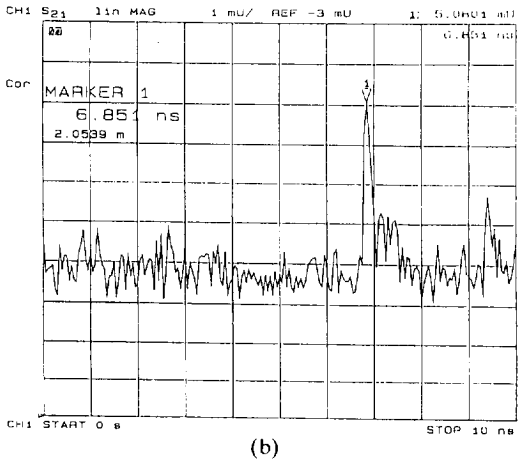

(b)

Fig. 3. Pulse delay measurement for the odd (a) and even (b) quasi-TEM modes.

Table 1
Experimental parameters

Electron beam		
energy	<11	[keV]
current	~0.5	[A]
pulse width	<1	[ms]
Magnetic field		
solenoid	2.5–3	[kG]
folded-foil undulator:		
strength	<0.1	[kG]
period	2	[cm]
Waveguide		
rectangular tube	0.9×0.4	[in.^{2}]
metal striplines:		
cross-section	2×3	[mm]
gap	11	[mm]
dielectric slabs:		
cross-section	0.2×0.4	[in.]
dielectric constant	140	
cavity length	18	[in.]

tion to the dielectric slabs from the electron beam. The stripline dielectric waveguide is described in Section 2. The experimental setup and results are presented in Sections 3 and 4, respectively.

2. The stripline dielectric waveguide

The dielectric-loaded stripline waveguide used in our experiment is shown schematically in Fig. 1. It consists of two copper strips laid along a standard WR90 rectangular metallic tube. Each copper strip is attached to a dielectric slab along the waveguide wall. The dielectric slabs are made of ceramic (MCT-140, manufactured by Trans-Tech

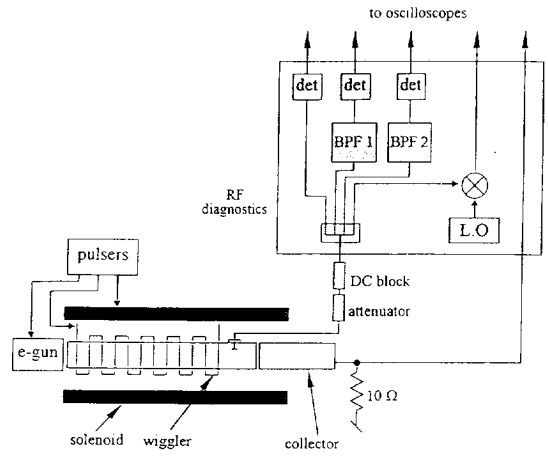

Fig. 4. The diagnostic setup of the dielectric-loaded FEM oscillator experiment.

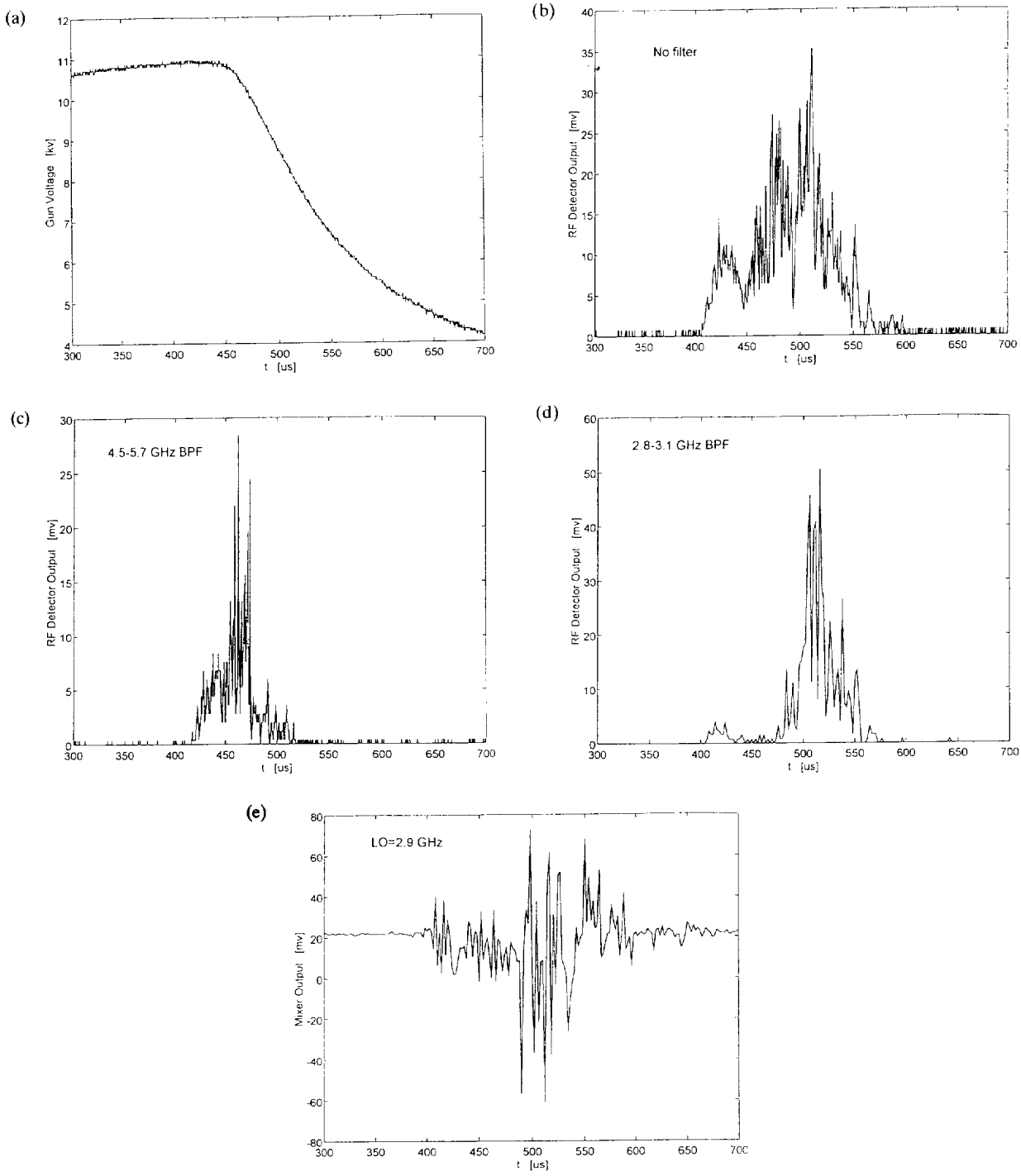

Fig. 5. Typical experimental measurements. (a) The electron gun voltage. (b) The RF detector output (no filter). (c) The detected output of the 4.5–5.7 GHz bandpass filter. (d) The detected output of the 2.8–3.1 GHz bandpass filter. (e) The hetrodyine mixer output with a 2.9 GHz local oscillator.

Ceramics Inc.) with a dielectric constant of $\varepsilon \approx 140$. The metal strips have both mechanical and electrical functions; they protect the dielectric material from the electron beam and prevent electrical charges and damage to the dielectric slabs. In addition, they support quasi-TEM modes without a cut-off frequency.

The double stripline waveguide shown in Fig. 1 supports even and odd quasi-TEM modes. Each mode has a different transverse field profile as shown in Figs. 2a and 2b, and it propagates in a different phase velocity according to its specific effective dielectric constant ε_{eff}. The delay time of each mode is measured in the time-domain by an HP 8720A vector-network analyser. The even and odd modes are excited separately by appropriate transitions from a coaxial line to the stripline waveguide. Figs. 3a and 3b show the delay time of short pulses along the waveguide in even and odd TEM modes. The effective dielectric constants resulting from these measurements are $\varepsilon_{eff} \approx 8$ for the odd mode, and $\varepsilon_{eff} \approx 150$ for the even mode.

3. Experimental set-up

The dielectric-loaded waveguide shown in Fig. 1 is installed in the low-energy FEM and CRM experimental setup at Tel Aviv University [15]. The device consists of a thermionic Pierce electron gun, a WR90 waveguide, and a solenoid. In this experiment we use a planar coaxially-fed folded-foil undulator as described in Ref. [16]. The 10 keV electron beam is dumped at the exit of the interaction region onto a collector, which is also used to measure the electron current. Three synchronized pulsers generate the solenoid, the e-gun, and the wiggler pulses, as described in Ref. [17]. The experimental parameters are listed in Table 1.

The oscillator cavity consists of the dielectric-loaded stripline waveguide shown in Fig. 1. The waveguide is terminated at both ends by two partial mirrors with holes at the centers for the entrance and exit of the electron beam. A small probe placed in the cavity couples −25 dB of the inside radiation power to the output connector. The sampled RF power is attenuated and split into two parallel bandpass filters (BPFs) as shown in Fig. 4. Another portion of the output power is mixed with a local oscillator (LO) and produces the intermediate frequency (IF) signal. The detected outputs of the filters and the IF signal are traced by a Tektronix TDS540 and TDS620 digital oscilloscopes. This diagnostic setup measures the spectral evolution of the oscillator radiation simultaneously with the e beam voltage and current, and the solenoid and wiggler fields.

4. Experimental results

Typical measurements of the stripline dielectric-loaded FEM oscillator are presented in Figs. 5a–5e. The sweep in the electron gun voltage is shown in Fig. 5a. The corresponding measurement of the RF detector output without filtering is shown in Fig. 5b. A burst of RF radiation is observed in a wide range of electron energies from 11 to 6 keV. The spectral evolution of the oscillations is measured by the two BPFs and by the heterodyne mixer. Figs. 5c and 5d show the detected outputs of the BPFs in the ranges 4.5–5.7 GHz and 2.8–3.1 GHz, respectively. The results show a frequency shift from high to low frequencies during the pulse, in accordance with the electron energy sweep. The output of the high BPF appears at the beginning of the RF burst whereas the low BPF output appears at its end. The latter is confirmed by the IF signal for an LO frequency of 2.9 GHz (within the range of the low BPF) which appears at the same time.

Similar results are obtained in a range of axial magnetic fields from 2.5 to 3 kG (the corresponding cyclotron frequency is 7–8 GHz, respectively). No emission of radiation is observed without the wiggler field in this experiment, hence, the measured effect is considered as an undulator-beam interaction with slow waves.

5. Conclusions

The feasibility of a slow-wave FEL interaction implemented in a stripline structure is demonstrated in this experiment. The effect of the dielectric-loaded waveguide on the FEL interaction is shown in the tuning diagram in Fig. 6. It shows the slow-wave line for the odd mode in our experiment intersecting with the electron beam line in the energy range from 11 to 6 keV. The dielectric loading increases the em-wave frequency (as compared to a free-space interaction with the same energy) and broadens its bandwidth. This tuning diagram based on Eq. (2) does not take into account space-charge and axial-magnetic field effects which may vary the tuning condition. Therefore it products slightly higher frequencies than observed in the experiment. However, the effect of increasing the Doppler

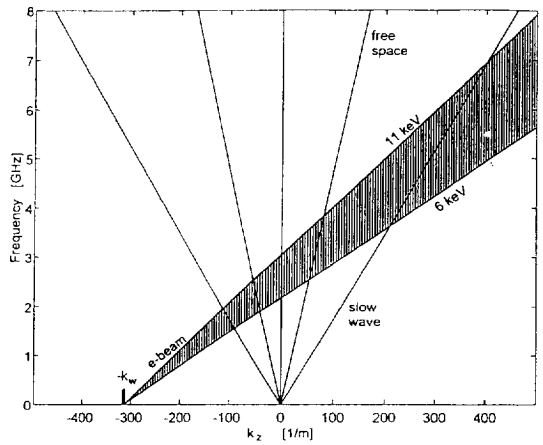

Fig. 6. The tuning diagram of the FEL interaction with slow waves.

up-shift due to the dielectric loading is clearly seen in this experiment.

Acknowledgements

This research is supported in parts by the Israeli Ministry of Energy, the Belfer Center for Energy Research, the Israeli Ministry of Science, and the Israeli Academy of Science.

References

[1] L.R. Elias, W. Fairbank, J. Madey, H.A. Schwettman and T. Smith, Phys. Rev. Lett. 36 (1976) 717.
[2] R.M. Phillips. IRE Trans. ED-7 (1960) 231; see also Nucl. Instr. and Meth. A 272 (1988) 1.
[3] J. Feinstein, A.S. Fisher, M.B. Reid, A. Ho, H.D. Dulman and R.H. Pantell, Phys. Rev. Lett. 60 (1988) 18.
[4] G. Bekefi, J.S. Wurtele and I.H. Deutsch, Phys. Rev. A (1986) 1228.
[5] A.H. Ho, J. Feinstein and R.H. Pantell, IEEE J. Quantum Electron. QE-23 (1987) 1545.
[6] E. Jerby, Phys. Rev. A 44 (1991) 703.
[7] J.E. Walsh, T.C. Marshall and S.P. Schlezinger, Phys. Fluids 20 (1977) 709.
[8] G.P. Fomenko, A.G. Pelyodov, A.S. Shlapakovskii and Yu.G. Shtein, Nucl. Instr. and Meth. A 331 (1993) 152.
[9] T. Taguchi and K. Mima, Nucl. Instr. and Meth. A 331 (1993) 597.
[10] K.C. Leou, D.B. McDermott and N.C. Luhman, Jr., IEEE Trans. Plasma Sci. 20 (1992) 188.
[11] A.K. Ganguly and S. Ahn, Phys. Rev. A 42 (1990) 3554.
[12] Ling Gen-shen and Liu Yong-gui, Phys. Rev. E 50 (1994) 4262.
[13] G. Mishra, K.P. Maheshwari and G. Praburam, IEEE Trans. Plasma Sci. 21 (1994) 181.
[14] T. Shiozawa and M. Mikawa, IEEE J. Quantum Electron. QE-30 (1994) 2676.
[15] R. Drori, E. Jerby and A. Shahadi, Nucl. Instr. and Meth. A 358 (1995) 151.
[16] A. Sneh and E. Jerby, Nucl. Instr. and Meth. A 285 (1989) 294.
[17] E. Jerby, A. Shahadi, V. Grinberg, V. Dikhtiar, M. Sheinin, E. Agmon, H. Golombek, V. Trebich, M. Bensal and G. Bekefi, IEEE J. Quantum Electron. QE-31 (1995) 970.